Symmetrical analysis of the defect level splitting in two-dimensional photonic crystals

2003 J. Phys.: Condens. Matter 15 4535

(http://iopscience.iop.org/0953-8984/15/26/303)

INSTITUTE OF PHYSICS PUBLISHING JOURNAL OF PHYSICS: CONDENSED MATTER

J. Phys.: Condens. Matter **15** (2003) 4535–4542 PII: S0953-8984(03)59301-8

Symmetrical analysis of the defect level splitting in two-dimensional photonic crystals

N Malkova, S Kim and V Gopalan

Materials Research Institute, Pennsylvania State University, University Park, PA 16802, USA

Received 6 February 2003, in final form 13 May 2003
Published 20 June 2003
Online at stacks.iop.org/JPhysCM/15/4535

Abstract

In this paper doubly degenerate defect states in the band gap of the two-dimensional photonic crystal are studied. These states can be split by a convenient distortion of the lattice. Through analogy with the Jahn–Teller effect in solids, we present a group theoretical analysis of the lifting of the degeneracy of doubly degenerate states in a square lattice by different vibronic modes. The effect is supported by the supercell plane-wave model and by the finite difference time domain technique. We suggest ways for using the effect in photonic switching devices and waveguides.

Photonic crystals are of importance for numerous applications involving light modulation [1]. One such useful system based on photonic crystals is the high-Q photonic band gap (PBG) resonant cavity that can be realized by introducing a point defect into an otherwise regular photonic lattice which induces the existence of exponentially decaying states that appear within the stop band.

Interest in the construction of *active tunable* elements has led to the idea of introducing interactions into an otherwise perfect periodic photonic crystal. Interaction effects in the photonic crystals may be realized in two ways. The first is the coulombic interaction which, in the case of the photonic crystal, implies nonlinear optical behaviour [2]. Another possible interaction is photon–vibration interaction, which should appear in a photonic crystal subject to mechanical vibrations [3]. It has been reported [4] that tuning the driving frequency of vibrations to the frequency of interband transition leads to coupling of the optical modes.

In this paper we propose yet another principle that is potentially useful in the design of active elements. In particularly, we are interested in splitting the degeneracy of the defect state by means of Jahn–Teller distortion of the lattice. The splitting of a degenerate state by some lowering symmetry perturbation is well known. For two-dimensional photonic crystals this was discussed in [5]. The aim of this paper is to study the splitting of the degenerate defect state due to Jahn–Teller distortion of the lattice and to give insight into the tuning characteristic of the defect mode.

A close analogy between defect electron states in the energy band gap of semiconductors and defect states inside the photon band gap of the defect photonic crystals allows one to expect

the Jahn–Teller effect in photonic crystals. The first step is to present Maxwell's equations for a photonic crystal subject to vibrations with a driven frequency ω in a Schrödinger-like form $\mathrm{i}\frac{\partial}{\partial t}\boldsymbol{\Psi} = \mathcal{H}\boldsymbol{\Psi}$, where we define a wavefunction and Hamiltonian $\mathcal{H}$ as

$$\boldsymbol{\Psi} = \begin{bmatrix} \boldsymbol{D} \\ \boldsymbol{H} \end{bmatrix}, \qquad \mathcal{H} = \begin{bmatrix} 0 & \mathrm{i}\boldsymbol{\nabla}\times \\ -\mathrm{i}\boldsymbol{\nabla}\times\frac{1}{\epsilon(\boldsymbol{r}+\boldsymbol{R}(t))} & 0 \end{bmatrix}. \tag{1}$$

Here we consider a magnetic neutral medium where $\mu = 1$, $\boldsymbol{D}$ is the electric displacement field, $\boldsymbol{H}$ is the magnetic field, and $\boldsymbol{R}(t)$ describes the displacement of the dielectric rods such that $\boldsymbol{R}(t) = \sum_l \boldsymbol{R}_l \mathrm{e}^{\mathrm{i}\omega t}$, where l goes over the all sites of the photonic lattice. In the first approximation of the perturbation theory we assume that the amplitude of the vibrations is much less than the lattice constant. We can then present the Hamiltonian $\mathcal{H}$ as a sum of the unperturbed Hamiltonian $\mathcal{H}_0$ and perturbation potential V:

$$\mathcal{H} = \mathcal{H}_0 + V = \begin{pmatrix} 0 & \mathrm{i}\boldsymbol{\nabla}\times \\ -\mathrm{i}\boldsymbol{\nabla}\times\frac{1}{\epsilon(\boldsymbol{r})} & 0 \end{pmatrix} + \begin{pmatrix} 0 & 0 \\ \mathrm{i}\boldsymbol{\nabla}\times\frac{\delta\epsilon}{\epsilon(\boldsymbol{r})^2} & 0 \end{pmatrix}, \tag{2}$$

where $\delta\epsilon = \frac{\partial\epsilon}{\partial\boldsymbol{r}}|_0 \boldsymbol{R}(t)$ (the index 0 shows that the derivative is taken at zeroth displacement). In the frame of time-dependent perturbation theory for non-Hermitian perturbation potential V [3], we are interested in removing the degeneracy of a defect state due to coupling with the vibronic mode. So, we are looking for a solution of the Schrödinger equation as an extension over unperturbed states $\Psi_i^{(0)}$ that describes the degenerate state with frequency ω_0, i.e. $\Psi = \sum_i a_i(t)\Psi_i^{(0)}$, where $a_i(t)$ are time-dependent coefficients. We arrive at

$$\mathrm{i}\frac{\partial a_j(t)}{\partial t} = \sum_i a_i(t) V_{ij} \mathrm{e}^{\mathrm{i}\omega t}, \tag{3}$$

where $V_{ij} = \langle\Psi_i^{(0)}|V|\Psi_j^{(0)}\rangle = -\omega_0 \int \frac{\delta\epsilon}{\epsilon}\boldsymbol{H}_i^{(0)*}\cdot\boldsymbol{H}_j^{(0)}\,\mathrm{d}\boldsymbol{r}$. Since all $\Psi_i^{(0)}$ wavefunctions represent just the same energy state, the resonance condition will be the case if the driven frequency $\omega = 0$. This corresponds to a frozen vibronic mode. But this effect will be realized if and only if the matrix elements V_{ij} do not equal zero.

To be more specific, we consider a two-dimensional photonic crystal with a square lattice of dielectric rods in vacuum and doped by a defect rod that is characterized by a radius of different magnitude. The point group symmetry of the square lattice is $\mathrm{C_{4v}}$. If the defect rod is localized in the site of the lattice then by symmetry it may be described both by one-dimensional $\mathrm{A_{1,2}}$, $\mathrm{B_{1,2}}$ and two-dimensional E irreducible representations of the group $\mathrm{C_{4v}}$ [6]. A one-dimensional irreducible representation results in a non-degenerate photon state. The two-dimensional representation results in a doubly degenerate state, which is the state to be considered here.

We consider a photonic crystal subject to vibrations. All lattice vibrations can be presented in terms of the normal coordinates as a sum of the normal irreducible vibrations α, then vibronic perturbation can be extended over normal vibrations $\delta\epsilon(\boldsymbol{r}) = \sum_\alpha \boldsymbol{R}_\alpha \cdot \frac{\partial\epsilon}{\partial\boldsymbol{r}}|_0$ [7]. Each normal vibration α is determined by the symmetrized displacements $\boldsymbol{R}_\alpha$ and the so-called deformation potential $\frac{\partial\epsilon}{\partial\boldsymbol{r}}$. By symmetrized displacements we mean collective (concerted) nuclear displacements which, under the symmetry operations of the molecular point group, transform according to one of its irreducible representations. They can be found easily using group theory methods. For a two-dimensional square lattice with the defect on a lattice site, by molecular we mean the cell composed of the dielectric rods nearest to the defect. In this case, there can be $2\mathrm{A_1}$, $\mathrm{B_1}$, $2\mathrm{B_2}$ and 2E normal irreducible vibrations of the lattice. The $\mathrm{A_1}$ normal vibration is a total symmetrical vibration, while the $\mathrm{B_1}$ and $\mathrm{B_2}$ modes are antisymmetrical normal vibrations described by one-dimensional irreducible representations [7]. The E mode of the normal vibrations are characterized by a two-dimensional irreducible representation with

the 1×2 basis vector, the components transforming one through another [7]. As follows from Jahn–Teller theorem [7], to split the doubly degenerate E photonic state the matrix element of the corresponding vibronic mode α is

$$V_{ij}^{\alpha} = -\omega_0 \int \boldsymbol{H}_i^{(0)E*}(\boldsymbol{r}) \cdot V(\boldsymbol{r}, \boldsymbol{R}_\alpha) \boldsymbol{H}_j^{(0)E}(\boldsymbol{r})\, \mathrm{d}\boldsymbol{r} \neq 0. \tag{4}$$

Here $V(\boldsymbol{r}, \boldsymbol{R}_\alpha) = \frac{1}{\epsilon} \boldsymbol{R}_\alpha \cdot \frac{\partial \epsilon}{\partial \boldsymbol{r}}$ is a perturbation potential caused by the corresponding normal vibrations α and described by the symmetry of the normal displacements. From the symmetry analysis, this matrix element is nonzero if and only if $\mathrm{E} \times \mathrm{E} = \alpha$. Since, $\mathrm{E}^2 = \mathrm{A}_1 + \mathrm{A}_2 + \mathrm{B}_1 + \mathrm{B}_2$, only the perturbations with the symmetry of the A_1, B_1 and B_2 normal vibrations can shift the degeneracy of the E defect mode.

In accordance with group theoretical analysis, the eigenvectors of the doubly degenerate E state are represented as two 1×2 column vectors with components that transform as vectors in the x and y directions. For electronic states in solids, they are usually presented as p_x and p_y orbitals. It is known [6] that the defect E modes have the shape of the p_x and p_y functions. Thus, we can specify the unperturbed wavefunctions of the E state as functions with the symmetry of p_x and p_y orbitals. In this case, the matrix elements of the vibronic perturbation with the symmetry of the α-mode are written as

$$V_{ij}^{\alpha} \sim \int p_i(\boldsymbol{r}) V(\boldsymbol{r}, \boldsymbol{R}_\alpha) p_j(\boldsymbol{r})\, \mathrm{d}\boldsymbol{r}. \tag{5}$$

For the case of the total symmetrical vibration A_1, $V_{xx}^{\mathrm{A}_1} = V_{yy}^{\mathrm{A}_1}$ and $V_{xy}^{\mathrm{A}_1} = 0$. Solving equation (2) with these matrix elements, we find that the interaction of the photonic E state with the A_1 vibration results in an equal shift of the doubly degenerate state without lifting the degeneracy. The situation is different for the case of the antisymmetric $\mathrm{B}_{1,2}$ modes. For the B_1 mode, $V_{xx}^{\mathrm{B}_1} = -V_{yy}^{\mathrm{B}_1}$ and $V_{xy}^{\mathrm{B}_1} = 0$. As a result, the degeneracy of the E-photonic mode is removed, resulting in two levels $\omega_{1,2}^{\mathrm{B}_1} = \omega_0 \pm V_{xx}^{\mathrm{B}_1}$. For the B_2 mode, $V_{xx}^{\mathrm{B}_2} = V_{yy}^{\mathrm{B}_2} = 0$ and $V_{xy}^{\mathrm{B}_2} = V_{xy}^{\mathrm{B}_2}$. This results in the two split levels $\omega_{1,2}^{\mathrm{B}_2} = \omega_0 \pm V_{xy}^{\mathrm{B}_2}$.

From this analysis we note the following. First, because of the linear dependence of the perturbative potential on the amplitude of vibration ($V_{ij}^{\alpha} \sim |\boldsymbol{R}_\alpha|$), the splitting of the doubly degenerate level should show a linear scaling with the magnitude of the lattice distortion through a scaling coefficient called the constant of vibronic coupling (or vibronic constant). Second, vibronic constants corresponding to different vibronic modes α are determined by different matrix elements V_{ij}^{α}. For the case of the B_1 mode, this is a diagonal matrix element $V_{xx}^{\mathrm{B}_1}$. For the B_2 mode, the splitting is determined by the non-diagonal matrix element $V_{xy}^{\mathrm{B}_2}$. It is natural to expect that the relative magnitudes of the shift of the defect mode will be greater for the case of the coupling defect state for the B_1 mode than for the B_2 mode.

Now, we provide numerical support for the static Jahn–Teller effect. We will present supercell plane-wave and finite difference time domain (FDTD) calculations of the two-dimensional defect crystal. As a model crystal we consider a square photonic crystal of dielectric rods, embedded in air, with lattice constant a, rod radius $r = 0.2a$ and dielectric constant $\epsilon_r = 11.9$. Here, only modes with odd (TM-like) symmetry are considered, since this is the symmetry of the bands that exhibit a gap for the square lattice. We study the defect state created by the defect rod with radius $r_d = 0.3a$ and the same dielectric constant $\epsilon_d = 11.9$ as the other rods. Namely, we are interested in the doubly degenerate defect state that, in this case, lies inside the first band gap. To simplify analysis of the effect studied, we take the amplitudes of the rod dispacements $|\boldsymbol{R}_\alpha|$ as being non-zero for only the nearest neighbours of the defect rod. We consider distortions of the lattice within the limits $\Delta r = 0$–$0.3a$, keeping in mind that only small distortions ($\Delta r \ll a$) allow application of the linear approximation of the vibronic potential (equation (2)).

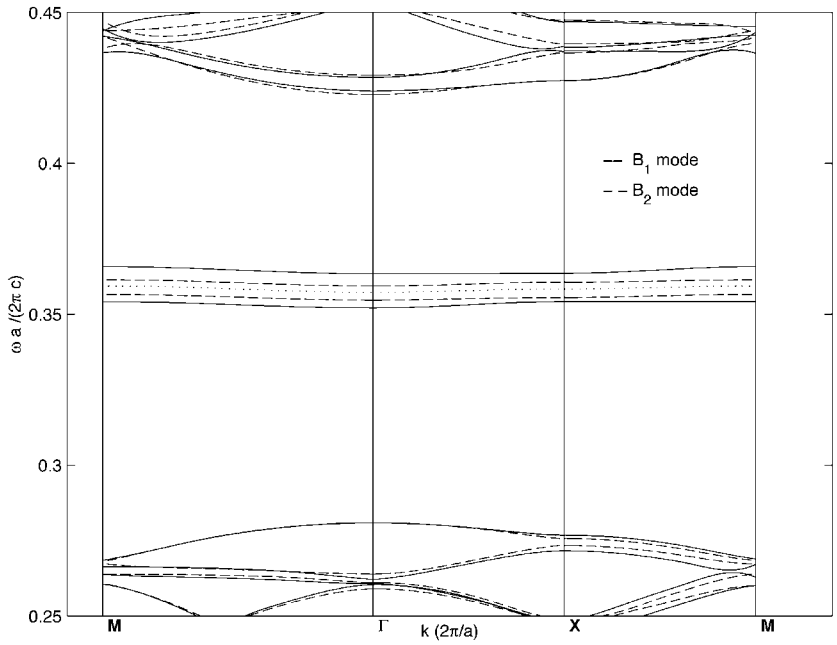

Figure 1. The supercell plane-wave spectrum of the defect photonic crystal coupled with the B_1 (solid curve) and B_2 (dashed curve) vibronic modes for rod displacement magnitude $\Delta r = 0.1a$. The dotted curve shows the doubly degenerate defect level in the unperturbed system.

The supercell plane-wave calculations of the defect state have been performed using the usual technique [8]. To test our data, we worked with supercells that included 8 and 16 rods. The calculations were performed with $N = 1225$ plane waves. For frequencies inside the first band gap, the data showed good convergence and relative error less than 1%. Small dispersion (<0.05%) of the impurity band provides evidence for the small overlap between defect modes in the neighbouring cells.

In figures 1 and 2 we present the supercell plane-wave calculations of the static Jahn–Teller splitting effect for the $B_{1,2}$ vibronic modes. Figure 1 shows the plane-wave spectrum of the defect mode for a magnitude of distortion $\Delta r = 0.1a$. The dotted line shows the defect level in the unperturbed system. Figure 2 presents the distribution of the electric field for both the split states, for the cases of B_1 mode (a), (b) and B_2 mode (c), (d). The Jahn–Teller cell with nearest-neighbour displacements corresponding to the central defect is shown in figure 2.

To get the defect spectrum using the FDTD technique [9], we have followed the approach developed in [10]. Our computational domain contained 7×7 unit cells, with the defect localized at the centre. Each unit cell was divided into 20×20 discretization grid cells. The computational domain was surrounded by perfect matched layers, with a thickness corresponding to ten layers of the discretization grid. The total number of time steps was 80 000, where each time step $\Delta t = 1/(2\Delta xc)$. To ensure the convergence of our data, especially for small distortions of the lattice, we have performed calculations for a cell divided into 40×40 discretization grid cells. For this case, the number of perfectly matched layers was taken to be 20 layers of the discretization grid. The total number of time steps was 200 000. The analysis showed that the error in our calculations is less than 1%.

The FDTD calculations of the defect level splitting due to static Jahn–Teller distortion are shown in figure 3. We present the Fourier transform of the transmission spectrum intensity

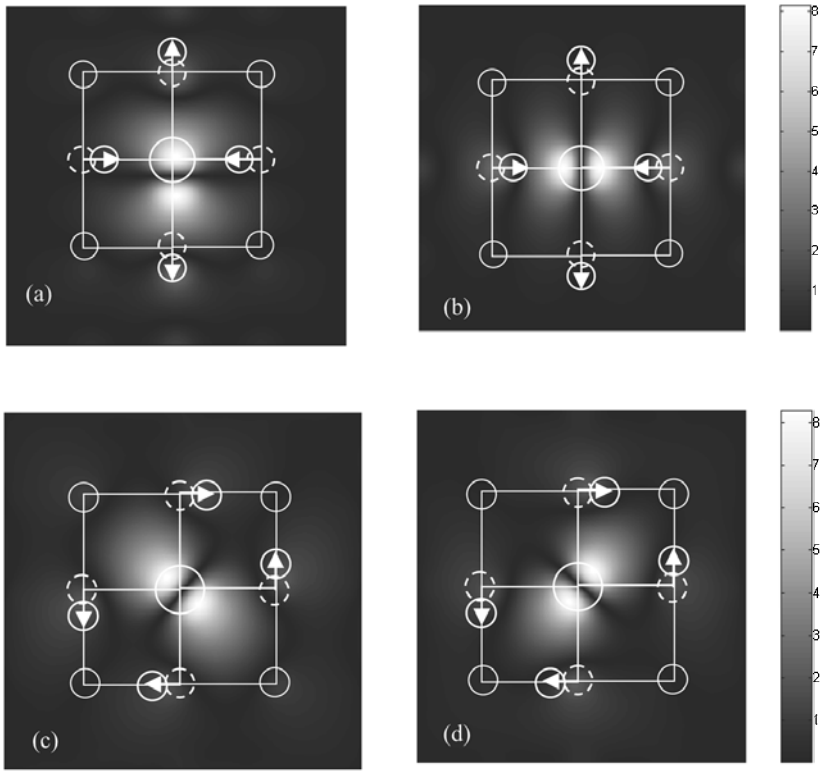

Figure 2. The distribution of the electric field intensity for two split defect modes: for the cases of coupling with the B_1 mode (a), (b) and B_2 mode (c), (d). The Jahn–Teller cell with nearest-neighbour displacements corresponding to the central defect is shown.

for the defect mode's Jahn–Teller splitting through the B_1 and B_2 modes for a magnitude of distortion $\Delta r = 0.1a$. The defect spectrum of the unperturbed system ($\Delta r = 0$) is shown by the dotted curves. The corresponding distributions of electric field for the two split modes are the same as that from the supercell plane-wave calculation (figure 2) and are therefore not repeated here. Since the intensity of the electric fields is symmetrical with respect to the Cartesian x- and y-axes (figure 2), centred on the defect, the Fourier amplitude of the defect spectrum depends on the point where the output data is collected. For example, for the B_1 mode, if we collect the data on the x axis, then only the p_x state is manifested in the Fourier spectrum (figure 3, dashed curve). If we collect the data on the y-axis, only the p_y state is noted (figure 3, dashed–dotted curve). If the collecting point is selected on the line $x = y$, then both p_x and p_y states are seen in the defect spectrum. In this case, the Fourier spectrum overlaps completely with both peaks.

For the case of the B_2 mode, the field distributions of the electric field are directed along $x = y$ and $-y$ lines (figures 2(c), (d)). So, if we are watching the defect spectrum on the line $x = y$, then we can see only the state with field distribution directed along $x = y$ line (figure 3, dashed curve). If we collect the data on the $x = -y$ line, then we can see only the state directed along $x = -y$ line (figure 3, dashed–dotted curve). Finally, if we collect the data at any other point (e.g. on the curve $x = 0$) then we can see both these states. We conclude that it is possible to manipulate the symmetry of the split photonic states of the defect

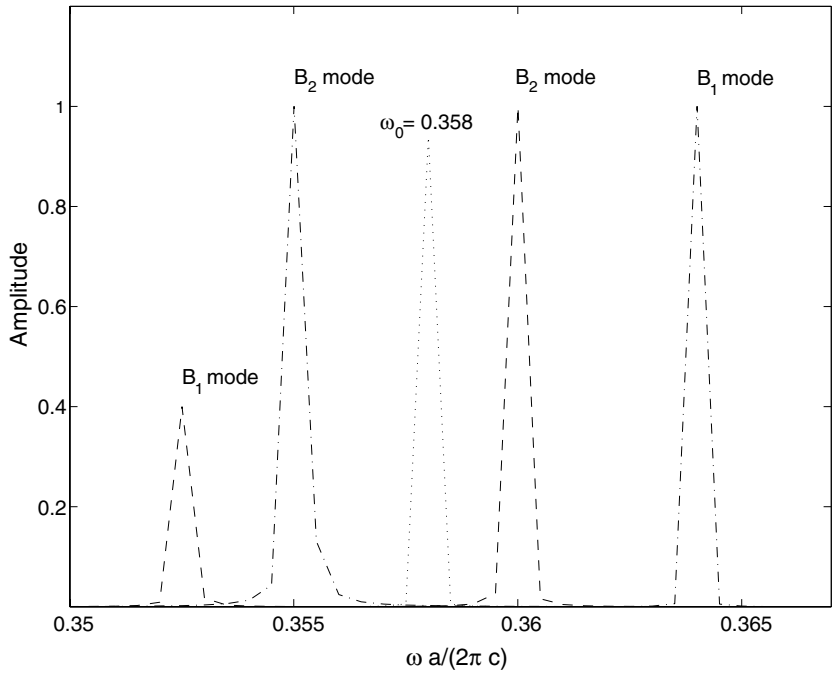

Figure 3. FDTD calculations of the defect photonic crystal coupled with the B_1 and B_2 vibronic modes for a rod displacement magnitude of $\Delta r = 0.1a$. The Fourier spectrum of the defect states coupled with the B_1 (B_2) mode, shown by the dashed and dashed–dotted curves, correspond to the data collecting points on the x-axis (the curve $x = y$) and y-axis (the curve $x = -y$), respectively.

level by choosing (a) appropriate distortion of the nearest neighbours (B_1 or B_2 modes) and (b) appropriate points for collecting data.

Figure 4(a) shows the dependence of the defect mode's frequency splitting on the relative amplitude of the distortion for the B_1 and B_2 modes. Here we present the data obtained using the supercell plane-wave technique (dashed lines) and the FDTD calculations (solid line). First, we note that the data calculated using both techniques are in reasonable agreement. Second, the tangent of the slope angle gives the vibronic constant. We note that the relative slope of the curve for the B_1 mode is two and half times greater than that for the B_2 mode. This supports our expectation that the diagonal matrix element $V_{xx}^{B_1}$, which determines the splitting by the B_1 mode, should be larger than the non-diagonal matrix element $V_{xy}^{B_2}$, which determines the splitting by the B_2 mode. Third, the magnitude of the defect level splitting shows a fairly linear scaling with distortion amplitude for both the perturbations. This is an obvious consequence of the linear approximation of the vibronic potential, which is valid for small distortions of the lattice. It is worth mentioning that, in spite of the fact that coupling of the defect state with the E vibronic mode is forbidden by symmetry in the first approximation of the perturbation theory (including only linear terms in the expansion of the vibronic potential), it however does exist in the second approximation when the second-order vibronic terms $V^{(2)} \sim \frac{\partial^2}{\partial r^2}(\frac{1}{\epsilon})R^2$ are included. In this case, the defect level splitting is proportional to the square of the distortion amplitude. The dependence of the defect mode's frequency splitting on the square of the distortion's relative amplitude for the E vibronic mode is shown in figure 4(b). We note that the defect level splitting appears only for a relatively large lattice distortion ($0.1a < \Delta r < a$) and shows linear scaling with the square of the distortion. The disagreement between the plane-wave and

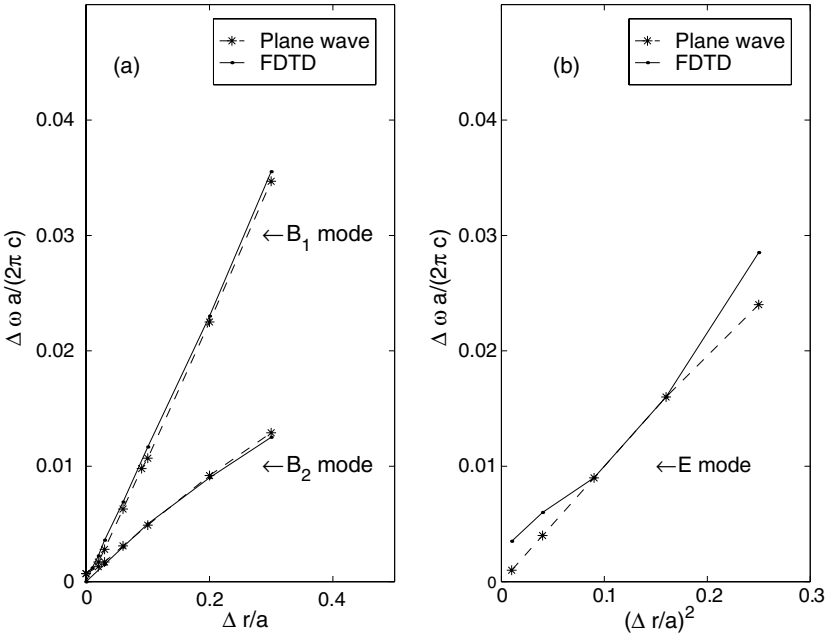

Figure 4. The dependence of the doubly degenerate defect state's frequency splitting on the relative amplitude of the distortion for the case of coupling the defect state with the $B_{1,2}$ (a) and E (b) vibronic modes. The data obtained from the supercell plane-wave and FDTD calculations are shown by dashed and solid lines, respectively.

FDTD calculations noticeable in figure 4(b) is a consequence of the poor convergency of the FDTD technique for the E mode. A better agreement between the plane-wave and FDTD data should be achieved with a finer FDTD grid.

In this paper we have studied the effect of splitting the doubly degenerate defect level of a square two-dimensional photonic lattice using Jahn–Teller coupling with lattice vibrations. In the static approximation, the effect shows a linear scaling of the magnitude of the frequency splitting with the amplitude of the lattice distortion. The symmetry of the split photon defect mode is shown to be driven by the symmetry of the lattice distortion or the corresponding vibronic mode. The condition for the effect, in the dynamic case, is that $V^{\alpha}\Delta r > K$, where K is the kinetic energy of the vibration determined by the amplitude of the displacement and the mass of the rods. As a matter of fact, the constant V^{α} determines the splitting of the states. We can estimate this from a tangent of the slope of curves in figure 4. For the case of the B_1 mode, the estimate gives $V \sim 0.1$ (in relative units). This requires that the velocity of the lattice vibrations should satisfy inequality $v^2 < 2(V\Delta r)/m$ (where v is the velocity of the vibrations and m is the mass of the rods). For the case of a photonic crystal with a nanometre-scale lattice subject to the B_1 vibration with amplitude $\Delta r/a = 0.1$, this indicates that the vibronic mode can be frozen in this case if $v < 10^4$ m s^{-1} and the frequency of the vibration $f < 10^6$ s^{-1}. In reconfigurable artificial photonic crystals, these parameters may be tuned to satisfy the above inequality.

In conclusion, we have described briefly possible applications of the Jahn–Teller distortion. Light incident on a photonic crystal with a square lattice and subject to the B_1 or B_2 vibrations will interact with all the appropriate defect states with field distributions that are non-orthogonal to the direction of propagation of the light in the lattice. The straightforward way to implement

the effect is to construct a photonic crystal on a piezoelectric substrate that gives the required distortion of the lattice near the defect [11]. This distortion could, for example, be used for optical switching or for improve guiding efficiency at the corners of sharp bends in optical waveguides. More sophisticated designs can include the coupling of elastic and electromagnetic waves in a lattice that is periodic in both dielectric and acoustic constants.

Acknowledgments

We would like to acknowledge support from the National Science Foundation Materials Research Science and Engineering Center and from ECS-9988685.

References

[1] Soukoulis C M (ed) 2001 *Photonic Crystals and Light Localization in the 21st Century (NATO ASI Series vol 563)* (New York: Kluwer–Academic)
[2] Scalora M, Bloemer M J, Manka A S, Dowling J P, Dowling C M, Bownden C M, Viswanathan R and Haus J W 1997 *Phys. Rev.* A **56** 3166
Tocci M D, Scalora M, Bloemer M J, Dowling J P and Bowden C M 1996 *Phys. Rev.* A **53** 2799
[3] Winn J N, Fan S and Joannopoulos J D 1999 *Phys. Rev.* B **59** 1551
[4] Skorobogatyi M and Joannopoulos J D 2000 *Phys. Rev.* B **61** 5293
Skorobogatyi M and Joannopoulos J D 2000 *Phys. Rev.* B **61** 15554
Konotop V V and Kuzmiak V 2001 *Phys. Rev.* B **64** 125120
[5] Painter O, Vuckovic J and Scherer A 1999 *J. Opt. Soc. Am.* B **16** 275
Loncar M, Yoshie T, Scherer A, Gogna P and Qiu Y 2002 *Appl. Phys. Lett.* **81** 2680
[6] Sakoda K and Shiroma H 1997 *Phys. Rev.* B **56** 4830
[7] Bersuker I B 1983 *The Jahn–Teller Effect and Vibronic Interactions in Modern Chemistry* (New York: Plenum)
[8] Meade R D, Brommer K D, Rappe A M and Joannopoulos J D 1991 *Phys. Rev.* B **44** 13772
[9] Taflove A and Hagness S C 2000 *Computational Electrodynamics: The Finite-Difference Time-Domain Method* (Boston, MA: Artech House Publishers)
[10] Qiu M and He S 2000 *Phys. Rev.* B **61** 12871
[11] Kim S and Gopalan V 2001 *Appl. Phys. Lett.* **78** 3015